Vol. 17, No. 3 (2018) 1173-1181
Revista Mexicana de Ingeniería Química

STUDY OF SILICA NANOCOMPOSITES FOR BUMPER FASCIA: MECHANICAL, CHEMICAL CHARACTERIZATION AND IMPACT SIMULATION

NANOCOMPOSITOS DE SILICE PARA FACIA: CARACTERIZACIÓN QUÍMICA, MECÁNICA Y SIMULACIÓN DE IMPACTO

P.A. Bravo-Carrasco[1], M. Salazar-Hernández[2], E.E Pérez-González[1], J.M. Mendoza-Miranda[1], H. Juárez-Rios[1], R. Miranda-Avilés[2], C. Salazar-Hernández[1]*

[1] *Unidad Profesional Interdisciplinaria de Ingeniería Campus Guanajuato, Instituto Politécnico Nacional, Av. Mineral de Valenciana No. 200 Col. Fracc. Industrial Puerto Interior, C.P. 36275 Silao de la Victoria, Guanajuato, México.*

[2] *Departamento de Ingeniería en Minas, Metalurgia y Geología, Universidad de Guanajuato, Ex Hacienda de San Matías S/N Colonia San Javier, C.P. 36020 Guanajuato, Gto, México.*

Received January 17, 2018; Accepted April 18, 2018

Abstract

Compound materials obtained by polyester resin reinforced with silica nanoparticles (RP/SiO_2) were characterized by different mechanical essays. Test tubes were obtained under ASTM norms with SiO_2 concentrations around 0.5 to 5% of weight. Compression tests indicated that silica nanoparticles lead to formation of ductile materials with respect to the polymer resin; compression deformation percentages (%ε) were determined around 45-52%; also, while the material resistance reached 90MPa. These materials showed a 38-67% increase in the bending module, and an increase of 16 to 34% in the absorption of impact energy. After mechanical characterization, was carried out a simulation of the mechanical behavior of bumper fascia made with the RP/SiO_2-A using finite element software. Frontal and lateral collision indicated a maximum stress around 21.5 MPa and 28.36 MPa respectively, these results suggested that the auto-part will only show plastic deformation in some areas; due to the elastic limit for RP/SiO_2 is 26 MPa and its maximum resistance at 89.8 MPa.

Keywords: Composite materials; SiO_2 nanoparticles; mechanical properties; simulation mechanical behavior.

Resumen

En este trabajo se caracterizó, mediante diferentes ensayos mecánicos, una familia de materiales compuestos empleando resina poliéster como matriz polimérica y nanopartículas de sílice como reforzante, (RP/SiO_2). Se obtuvieron las probetas de ensaye bajo las normas ASTM con diferentes concentraciones de SiO_2 (0.5 a 5% de peso); los ensayos de compresión indicaron que las nanopartículas de sílice promovieron la formación de materiales dúctiles con respecto a la resina polimérica; se determinaron porcentajes de deformación a compresión (% ε) entre 45 y 52%, mientras que la resistencia del material alcanzó 90MPa. Estos materiales mostraron un incremento entre 38 y 67% en el módulo de flexión y un aumento de 16 a 34% en la absorción de energía de impacto. Una vez realizada la caracterización mecánica, se realizó la simulación del comportamiento mecánico de un modelo de autoparte fabricado con el composito RP/SiO_2-A empleando un software de elemento finito. Se realizó una simulación de choque frontal y lateral registrándose un esfuerzo máximo de 21.5 MPa y 28.36 MPa respectivamente; estos resultados indican que la autoparte solo presentará deformación plástica en algunas zonas ya que el límite elástico del material es de 26 MPa y su resistencia máxima de 89.8 MPa.

Palabras clave: Resina poliéster, SiO_2-nanopartículas, propiedades mecánicas, simulación.

1 Introduction

A composite material (CM) is obtained through the physical mixture of two or more different types of materials, with the sole purpose of combining properties not present in the original materials. Therefore, new materials with unusual properties are created, such as high rigidity, conductivity, hardness and thermofluency, traction and corrosion resistance (Chawla KK, 2016; Gibson R.F, 2010; Sapuan S.M, 2017).

* *Corresponding author. E-mail*: msalazarh@ipn.com
Tel. (55) 57-29-60-00, Ext. 81378
doi: 10.24275/uam/izt/dcbi/revmexingquim/2018v17n3/Bravo
issn-e: 2395-8472

CM are constituted by a matrix or continuous phase which could be a metallic, polymeric or ceramic material. The other constituent of a composite is a scattered phase or reinforcing, and its main function lies in improving the matrix properties.

Composite materials due its excellent mechanical properties and low density have been employed in different industries such as automotive, aeronautic, construction, among others (Zaripov R, 2017; Karthigeyan P, 2017; Menna c, 2015; Olivas-Armendáriz I, 2009; González-Chi, 2007). In the automotive and aeronautic industries, lightweight structures are required for less energy consumption from the vehicle; thus composites such as the fiber reinforced polymer (GFRP): carbon fiber reinforced polymer (CFRP) and glass fiber reinforced polymer (GFRP) has been used at aircraft primary structural materials such as empennage, floor beams, fuselage (Nayak N.V, 2014). In automobiles, the composites are used in in different components, for example: car bonnet (Arasu P.M, 2014), automotive suspension systems (Morris C.J, 1986), roof car (Thoman M.R, 1999) etc. Also, these materials can be obtained used waste materials such as vegetal wastes (Cruz-Estrada RH, 2006) and henequen fiber (Balam-Cocom RJ, 2006).

However, the manufacturing methods conventional for FRP are the resin film infusion (RFI). In these methods the fiber is placed in racks and stretched into molds containing the shape of the desired part to be manufactured, on these molds the polymer resin is injected and when necessary vacuum is applied prior to injection of the polymer and heat to promote the curing. Commonly, automotive components are manufacturing by conformed.

Since 1994, Pinnavai et al, 1999; proposed the nanocomposite materials with the addition of nanostructured fillers like nano-clays, nano-oxides, carbon nanotubes and POSS, among others. In these materials, the nano-reinforcer or nano-filler is inserted on a molecular level among the chains of the polymeric matrix, reinforcing different properties such as mechanical resistance, thermic stability or electrical conductivity (Tang L. Ch, 2012; Azeez A.A, 2013; Constantinescu D.M, 2017; Pustak M, 2015).

The aim of present paper was the experimental study of the mechanical behavior of a family of nanoparticle-reinforced polyester unsaturated resin materials with various mechanical essays (hardness, compression, flexion and impact). Results of the mechanical resistance were employed to simulate, with commercial finite element software, the behavior of a bumper manufactured with RP/SiO_2 facing a frontal and lateral collision. The possibility to use these composites in auto parts manufacturing will be discussed in the results.

2 Materials and methods

2.1 PR/SiO_2 synthesis and its characterization

Several PR/SiO_2 composite materials were synthetized, chemical and mechanical characterized under a set of different tests. A brief summary of the synthesis process, test and test set-up for chemical and mechanical characteristics of the tested PR/SiO_2 composite materials are presented in the following sections.

2.2 PR/SiO_2 synthesis

Silica fume, SiO_2 (SIGMA, 200-300nm in aggregates) was employed as reinforce. The composites (PR-SiO_2) were synthesized using different proportions of reinforcer weight (see Table 1), industrial-grade unsaturated polyester resin (Poliforms, S.A.) and K-2000 catalyst were the starting materials to the polymeric matrix. A general methodology to obtain the PR-SiO_2 for the molding process was: A layer of mold release agent (polyvinyl alcohol, wax) was applied to the mold and drying for 5 min. Then, the unsaturated resin was mixed with the particle proportion (reinforcer) according to Table 1, after was added the catalyst (K-200) using a concentration of 5% weight of the polymer.

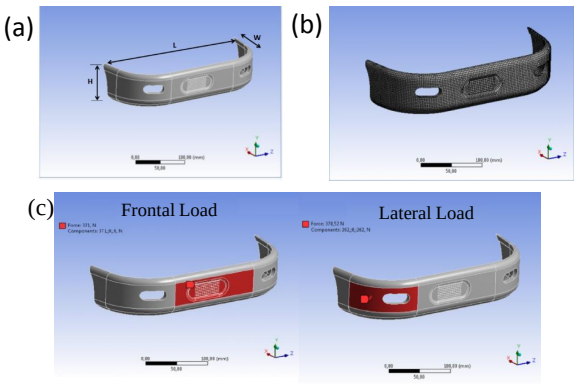

Fig. 1. (a) Isometric view of the bumper fascia model (b) final meshing condition (c) Frontal and lateral force applied on bumper fascia.

Table 1. PR-SiO_2 composition.

Compound Material	Reinforcer Proportion
	% weight SiO_2
RP-SiO_2-A	0.5
RP-SiO_2-B	1.0
RP-SiO_2-C	3.0
RP-SiO_2-D	5.0

This mixture was stirred until no more bubbles were formed, then poured in molds and left to cure at 50 °C for 24 hours.

2.3 Chemical Composition

The chemical composition for PR-SiO_2 was studied by attenuation reflection infrared spectroscopy (ATR-IR) using an ATR-Nicolet iS10 Thermo Scientific, measuring 600-4,000 cm^{-1}. An average of 32 scans was obtained with a resolution of 4 cm^{-1}. FTIR analyses allowed corroborating the physic modified at polyester resin due to silica nano-particles. Also, the composite materials morphology were observed by SEM using a JOEL-6510 plus.

2.4 Mechanical characterization

2.4.1 Leeb hardness test

The composites Leeb hardness (LH) was determined using a portable INSPEX durometer, model IPX-312. Ten readings were made and the data standard deviation estimated. The reference material used was bronze and the norm employed was ASTM-A956-06.

2.5 Compression and bending test

Ten samples for each PR/SiO_2 composition were tested under compression and bending test performed in the universal Shimazum II-Autograph AGS-J machine, using a deformation speed of 0.5 mm/min. The compression test was performed in accordance to the ASTM-D6108-13 norm and the bending test in accordance to the ASTM-D7264/D7264M-15 norm.

2.6 Impact test

Experimental impact tests were performed in a Charpy Diltecma DIT-PC410 pendulum using a 150N.m impact force. The dimensions and characteristics of all samples were set in accordance with the ASTM-D6110-10 norm.

2.7 Bumper fascia modeling and simulation

Bumpers are made from a metallic and plastic materials for application in the automotive industry, thus, they are considered structural as well as esthetic components. The stress and strain behavior for this automotive component could be predicted by a numerical simulation applying the finite element analysis (FEA); which is used by engineers and scientist to modeling and numerically solve very complex structural and fluid cases. Then, the use of FEA helps to reduce cost and time to study the design of components applying different materials and critical loads.

FEA enable the solution of Eq. 1; where $\{\vec{F}\}$ is a load vector, $[K]$ rigid matrix and $\{\vec{u}\}$ displacement vector. The result is the discretization of elements to obtain relationships between a set of displacements and forces.

$$\{\vec{F}\} = [K]\{\vec{u}\} \tag{1}$$

Table 2. PR-SiO_2 measured mechanical properties.

	Elastic module, E (MPa)	Compressive strength, σ_u (MPa)	Maximum deformation $\%\varepsilon$	Leeb Hardness, HL	Bending Module (MPa)	Impact Energy, J
Polyester Resin	6350 (± 60.2)	107.2 (± 5.8)	5.76 (± 5.8)	483 (± 20.8)	1110 (± 320)	2.5 (± 0.02)
PR/SiO_2-A	502.8 (± 40.5)	89.8 (± 6.2)	51.98 (± 1.5)	487 (± 13.5)	1696 (± 136)	3.11 (±0.54)
PR/SiO_2-B	643.1 (± 40.5)	85.9 (± 6.5)	50.36 (± 2.8)	478 (± 27.3)	1539 (± 305)	3.05 (±0.30)
PR/SiO_2-C	619.9 (± 70.9)	78.1 (± 7.4)	51.14 (± 7.4)	489 (± 20.2)	1537 (± 217)	3.36 (±0.42)
PR/SiO_2-D	681.6 (± 23.9)	76.1 (± 15.8)	45.38 (± 4.9)	509 (± 31.0)	1860 (± 244)	2.9 (0.27)

$$U_d = \frac{1+\vartheta}{3E}\left[\frac{(\sigma_x-\sigma_y)^2+(\sigma_y-\sigma_z)^2+(\sigma_z-\sigma_x)^2}{2}+6(\tau_{xy}^2+\tau_{yz}^2+\tau_{xz}^2)\right] \quad (2)$$

$$U_{d,sim} = \frac{1+\vartheta}{3E}\sigma_y^2 \quad (3)$$

$$\left[\frac{(\sigma_x-\sigma_y)^2+(\sigma_y-\sigma_z)^2+(\sigma_z-\sigma_x)^2}{2}+6(\tau_{xy}^2+\tau_{yz}^2+\tau_{xz}^2)\right]^{\frac{1}{2}} \geq \sigma_y \quad (4)$$

$$\left[\frac{(\sigma_x-\sigma_y)^2+(\sigma_y-\sigma_z)^2+(\sigma_z-\sigma_x)^2}{2}+6(\tau_{xy}^2+\tau_{yz}^2+\tau_{xz}^2)\right]^{\frac{1}{2}} \geq \sigma_v \quad (5)$$

Frequently, the Von Mises stress (σ_v) is obtained as solution to Eq (1). The concept of σ_v arises from the distortion energy failure theory. When a Cauchy stress tensor is applied on material; this absorbed an energy required for shape deformation. During pure distortion, the shape of the material change, but volume does not change; then is calculated the distortion energy per unit volume; U_d, Eq (2) that for simple tension case at the time of failure, this is calculate according to Eq (3).

According to distortion energy failure theory, the condition of failure is given by Eq (4); where the left side of the equation is denoted as Von Mises stress, σ_v; Eq (5). This condition is applied for isotropic and ductile materials, where the failure on materials occurs when the σ_v exceeds the elastic limit of the material ($\sigma_v \geq \sigma_y$).

2.8 Bumper simulation procedure

A numerical study has been conducted in order to explore the possibility of substituting the bumper fascia with PR-SiO_2 composite. Therefore, the stress and strain generated for a frontal and lateral crash in a bumper fascia was simulated using commercial software for FEM applying similar impact conditions reported by Alen et.al, 2014. The results of the simulation were obtained considering the mechanical properties determined for PR-SiO_2.

The CAD data of the bumper fascia was imported and the surfaces were created and meshed. The bumper fascia has basic dimensions (width, length, height and thickness) of 465 × 1700 × 300 × 8 mm, respectively. Fig. 1a shows the bumper fascia geometry used to generate the mesh. The computational mesh has been subsequently refined and a structured mesh of 68684 nodes and 16144 hexahedral and tetrahedral elements has been found to be sufficient to achieve mesh-independent solutions (Fig. 1b). The impact force was set on 8.67 kN and its was localized at the center and lateral of the bumper fascia (Fig. 1c) and the bumper fascia was fixed in laterals. Then, residuals are monitored and the solution is considered to converge when there are lower than 10^{-6}.

3 Results and discussion

The results obtained during various analyses (experimental test and numerical analysis) like chemical characterization, mechanical tests (compression, hardness, impact, bend analysis) and simulation of the PR-SiO_2 to manufacture a bumper fascia through a molding process, are presented in this section.

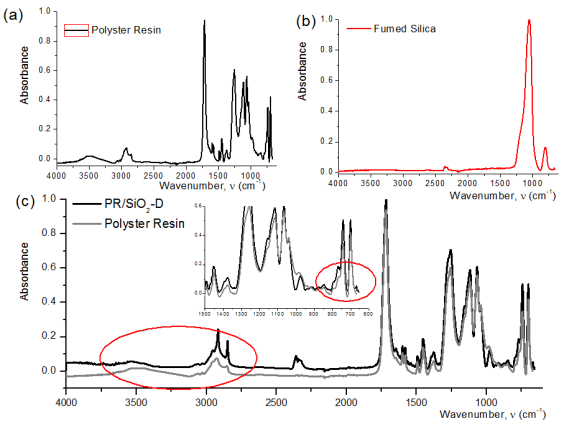

Fig. 2. Infrared spectroscopy silica composite materials.

Table 3. Mechanical properties prediction of RP/SiO_2 in relation with the reinforcer.

Mechanical	Property Function	R^2
Elastic module, E (MPa)	$y = -298472x^2 + 167.08x + 343$	0.9980
Maximum effort, σ_u (MPa)	$y = 8493x^2 - 764.5x + 93.12$	0.9978
% of maximum deformation (%ε)	$y = -5306.8x^2 + 167.08x + 50.4$	0.9075
Absorbed energy impact (J)	$y = -704.3x^2 + 36.15x + 2.87$	0.8167
Leeb Hardness (HL)	$y = 20486x^2 - 553.6x + 485.7$	0.9303
Maximum bending effort, σ_f (Mpa)	$y = -45141x^2 + 2948.9x + 10.34$	0.9980

y is the mechanical property, x is SiO_2 content in weight percentage

3.1 PR-SiO_2 chemical characterization

Fig. 2 shows the spectroscopy for starting materials and PR-SiO_2-D (5% SiO_2). Polyester is an unsaturated resin (Fig. 2a); hydroxyl group corresponding to acid group was observed at 3500 cm^{-1} (broad signal); aliphatic groups at 2850 cm^{-1} and 2933 cm^{-1} was small and broad signals (−CH2−; *v*as). Aromatic methylene groups (=C−H; *v*s) at 3062 cm^{-1} as a small signal (remarked with red circle). A 1715 cm^{-1} carbonyl was observed as a strong signal; acetate at 1257 cm^{-1} and aromatic ring at 1129-1065 cm^{-1} and 740-700 cm^{-1}. The fumed silica (Fig. 2b) is a silica free of water absorbed, only was observed the siloxane groups (Si−O−Si) at 1054 cm^{-1} (strong signal) and free-silanol groups (Si−OH) at 811 cm^{-1} (medium signal).

The spectra obtained for all composites were similar; Fig. 2c shown the corresponding to PR/SiO_2-D. Methylene group of the polymer resin was modified, observing fine signals (remarket with red circle); also, lightly slipping in all signals was observed.

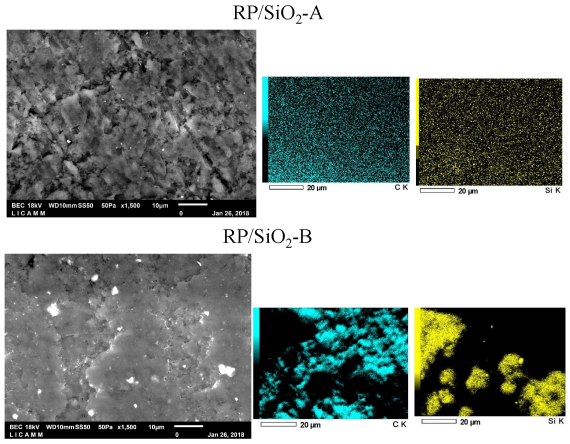

Fig. 3. Electronic microscopy for RP-SiO_2 composite materials.

Fig. 3 shown of electron microscopy for composites with minor and major silica concentration (RP/SiO_2-A and RP/SiO_2-D); the silica was embedded for polymer matrix; however, according to element mapping; a minor silica content the particles was homogeneously distributed in the polymeric resin, while increasing the silica content the silica cumulus were formed. Then, the silica distribution into the polymer could modify the mechanical properties for the composites.

3.2 RP-SiO_2 mechanical characterization

Fig. 4 shows the stress-strain curves for all RP-SiO_2 synthetized, displaying the typical behavior of a ductile material. The encircled area shows the elastic behavior and the arrow indicates a plastic behavior; while the polyester resin curve describes a rigid-brittle material σ_y, σ_u).

Table 2 summarizes the experimental mechanical characterization for PR-SiO_2 at compression, bending, hardness and Charpy impact tests.

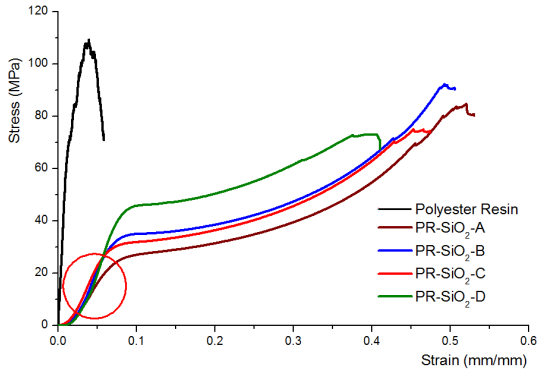

Fig. 4. RP-SiO_2 stress-strain Curve.

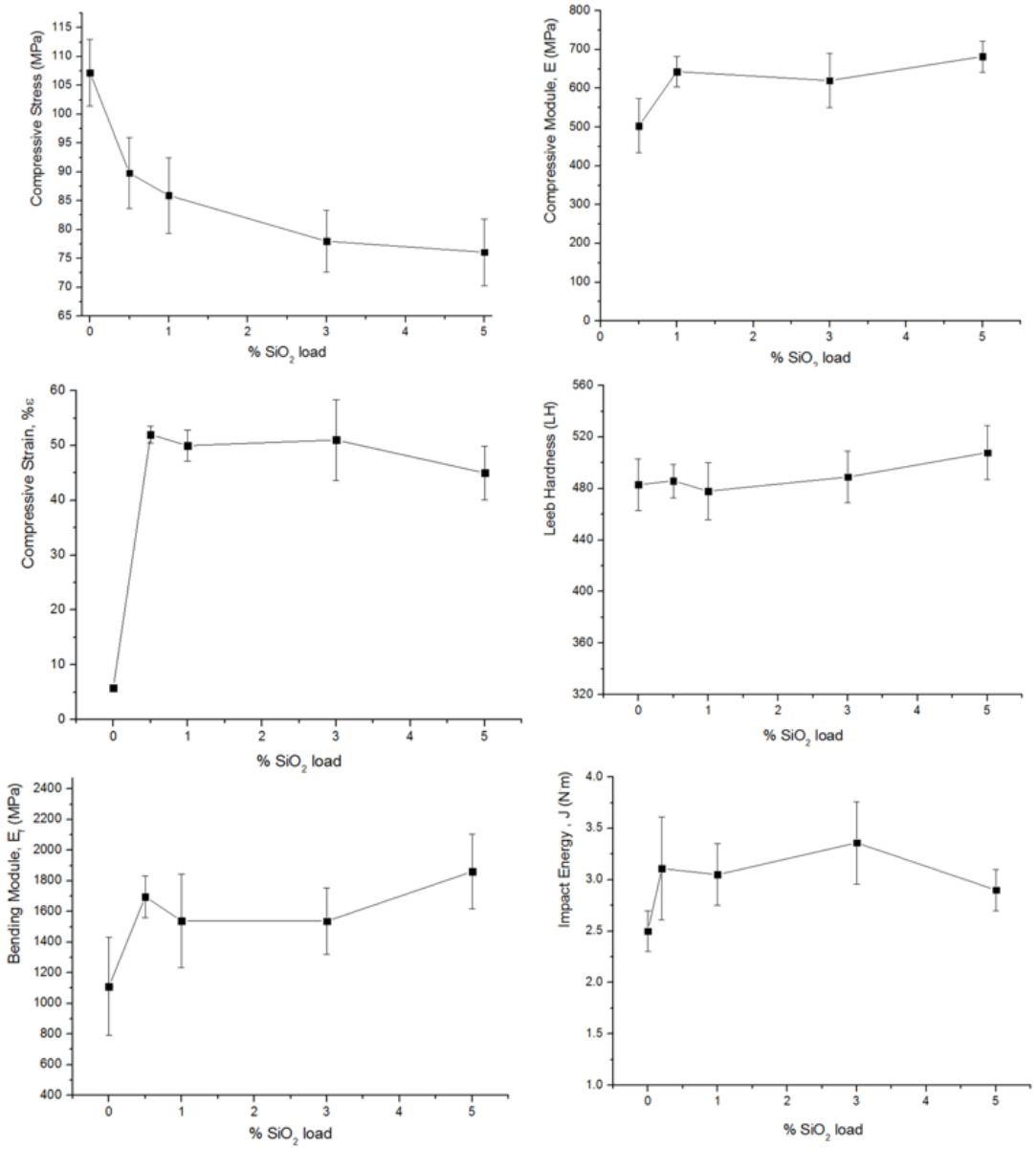

Fig. 5. Mechanical behavior of RP/SiO_2 in relation with silica content.

All assessment were carried out with ten probes; the results indicate a change in the material behavior forming compounds with ductile materials properties when silica is added to the polymer (E~500-643 MPa; $\%\varepsilon \sim$ 45-51), decreasing between 17 and 29% in the σ_u. The overall hardness of the material increased 5%. On the other hand, the addition of silica considerably modifies the polymere bending resistance; with an increase between 38.5% and 67.6%. Additionally, the impact force absorption increased between 16 and 34%. Fig. 5 shows the mechanical behavior of RP/SiO_2 in relation with the silica content in materials; these were adjusted to the linear and quadratic equations displayed on Table 3.

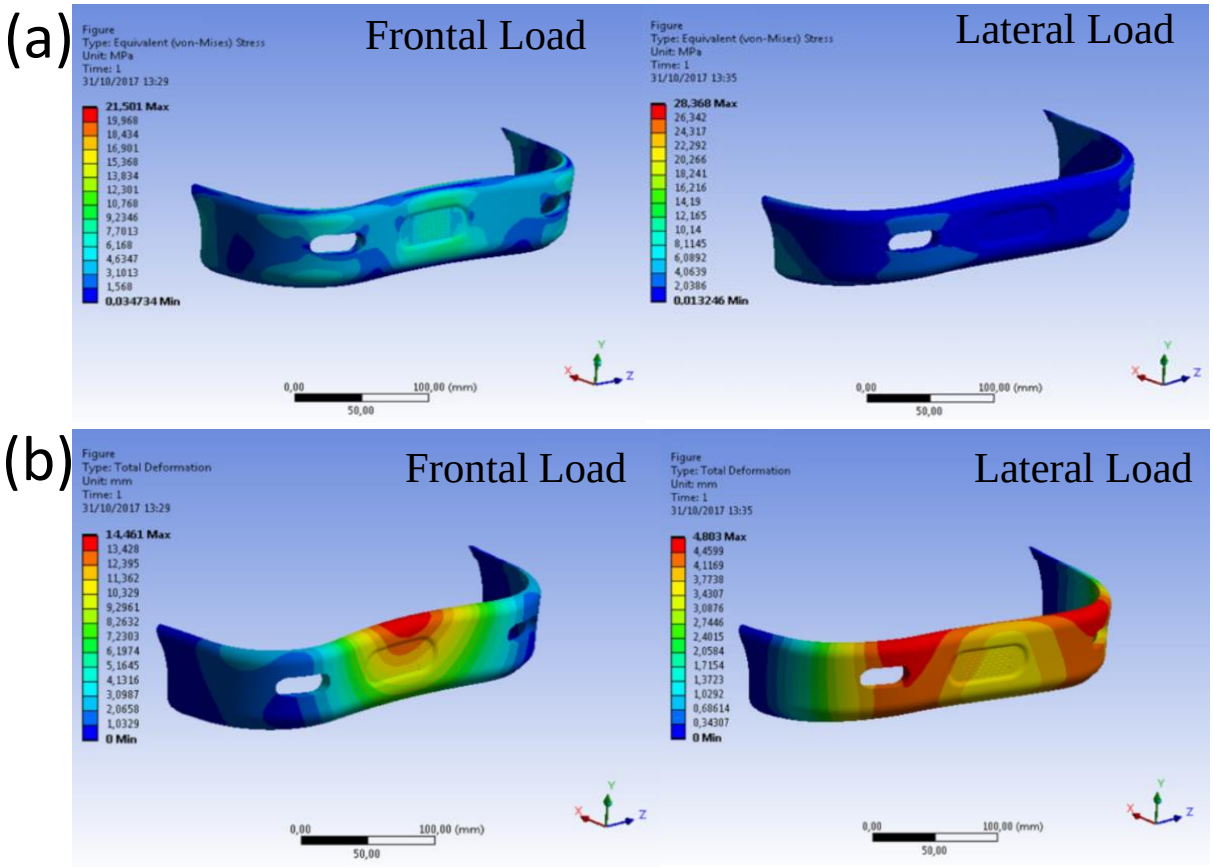

Fig. 6. Simulated PR/SiO_2 bumper fascia under frontal and lateral impacts (a) Von Misses stress distribution (b) deformation profile distribution.

These equations predict any mechanical property of the material (y variable) in accordance with the reinforcing content (x variable).

3.3 Simulation results of a bumper built with PR/SiO_2

According to the PR-SiO_2 mechanical behavior, PR/SiO_2-A was chosen for the bumper fascia simulation; Table 4 shows all properties used for the numerical simulation. In this part, the current bumper fascia was studied using the numerical model. After analysis it is observed that the maximum stress reached in frontal impact is 21.50 MPa, meanwhile for lateral impact the maximum stress reached is 28.36 MPa. Fig. 6a shows the stress distribution, according to the material properties experimentally obtained; there was no report of failure at any zone with the maximum stresses reached in frontal and lateral impact. This indicates that the bumper fascia could be sustaining the impact; however some region of the bumper fascia could present a plastic deformation when a lateral impact occurs due by the mechanical properties of the composite material. The distribution of the deformation when a frontal and lateral collision occurs is given in Fig. 6b. The maximum deformation reached is 14.46 mm and correspond to frontal impact.

Table 4. PR/SiO_2-A properties used for the crash impact simulation.

	Compound RP/SiO_2-A
Elastic module, E (MPa)	502.77
Maximum effort, σ_u (MPa)	89.80
Yield strength, σ_y (Mpa)	25.60
Density, ρ (g/cm^3)	1.30
*Material type	Isotropic

*Assuming isotropic materials with particle homogeneously distributed.

Conclusions

The addition of silica to the polyester resin modified the matrix mechanical behavior creating stronger materials. According to the results, silicon oxide concentrations under 5% created more ductile materials. Results from the impact test show that silica created materials with a higher energy adsorption capacity; such energy was estimated at 2.5 N•m for polyester resin, while Composite PR/SiO_2-A (0.5% SiO_2 weight) reached 3.11 N•m. On the other hand, given the effect of the added particles concentration on the mechanical properties of the compounds, it is safe to assure that no linear relation between these variables exists. A linear regression of these data produced quadratic functions for most mechanical properties (maximum resistance, σ_u; maximum deformation percentage, $\%\varepsilon$ and energy absorbed in impact, Ej). Additionally, to offer a more suitable material at lower cost and easier production, the modeling and simulation of a bumper fascia with the properties of PR-SiO_2-A (0.5% SiO_2 weight) was analyzed. Results of the frontal and lateral impact analysis show that the PR/SiO_2-A composite could be used for auto parts manufacture.

Acknowledgements

The authors wish to acknowledge the financial support of the Instituto Politécnico Nacional through grants SIP-20140844 and SIP-20150002.

Nomenclature

CM	Composite Materials
RP/SiO_2	Polyester resin reinforced with silica nanoparticle
RP/SiO_2-A	Polyester resin reinforced with 0.5% in weigh of silica nanoparticle
RP/SiO_2-B	Polyester resin reinforced with 1% in weigh of silica nanoparticle
RP/SiO_2-C	Polyester resin reinforced with 3% in weigh of silica nanoparticle
RP/SiO_2-D	Polyester resin reinforced with 5% in weigh of silica nanoparticle
E	Elastic module
σ_u	Maximum stress
$\%\varepsilon$	% of maximum deformation
EJ	Absorbed energy at impact
HL	Leeb Hardness
σ_f	Maximum bending stress

References

Alen J., Nidhi M.B. (2014). Modelling and analysis of an automotive bumper used for a low passenger vehicle. *International Journal of Engineering Trends and Technology 15*, 334-353.

Arasu P.M., Krishnaraj V., Rambabu B. (2014). Investigation of material and manufacturing process to develop high pedestrian safety composite bonnet. *Applied Mechanics and Materials 592-594*, 2518-2523.

Azeez A.A., Rhee K.Y., Park S.J., Hui D. (2013) Epoxy clay nanocomposites - processing, properties and applications: A review. *Composites Part B 45*, 308-320.

Balam-Cocom R.J., Duarte-Aranda S., Canché-Escamilla G. (2006) Obtention and characterization of composite of henequen "Pineapple" fibers and polipropilene. *Revista Mexicana de Ingeniería Química 5*, 39-44.

Chawla K.K. (2013). *Composite Materials Science and Engineering*, 3rd Ed. Springer, London.

Cruz-Estrada R.H., Fuentes-Carrillo P., Martínez-Domínguez O., Canché-Escamilla G., Carcía-Gómez C. (2006). Preparation of composite materials from vegetal wastes and high density polyethylene. *Revista Mexicana de Ingeniería Química 5*, 29-34

Constantinescu D.M., Apostol D.A., Picu C.R., Krawczyk K., Sieberer M. (2017). Mechanical properties of epoxy nanocomposites reinforced with functionalized silica nanoparticles. *Procedia Structural Integrity 58*, 647-652.

Gibson R.F. (2010). A review of recent research on mechanics of multifunctional composite materials and structure. *Composite Structures 92*, 2793-2810.

González-Chi P.I., Ramos-Torres W. (2007). Preparation and characterization of thermoplastic composite materials reinforced with engineering fiber. *Revista Mexicana de Ingeniería Química 6*, 51-58

Karthigeyan P., Senthil Raja M., Hariharan R., Karthikeyan R., Prakash S (2017). Performance evaluation of composite material for aircraft industries. *Materials Today Proceedings 4*, 3263-3269.

LeBaron P.C, Wang Z, Pinnavaia TJ (1999). Polymer layered silicate nanopomposites: an overview. *Applied Clay Science 15*, 11-29.

Menna C, Asprone D, Durante M, Zinno A, Balsamo A, Prota A (2015). Structural behaviour of masonry panels strengthened with an innovative hemp fiber composite grid. *Construction Building Materials 100*, 111-121.

Morris C.J. (1986). Composite integrated rear suspension. *Composite Structures 5*, 233-242.

Nayak N.V. (2014). Composite materials in aerospace applications. *International Journal of Scientific and Research Publications 4*, 238-247.

Olivas-Armendáriz I, García-Casillas P, Martel-Estrada A, Martínez-Sánchez R, Martínez-Villafañe A, Martínez-Pérez C.A. (2009). Preparation and characterization of chitosan/carbon nanotubes composites. *Revista Mexicana de Ingeniería Química 8*, 205-211.

Pustak M, Denac M, Leskovac L, Suab I, Musil L, Smit I. (2015). Polypropylene/silica micro and nanocomposite modified with poly(styrene-b-ethylene-co-butylene-b-styrene). *Journal of Applied Polymer Science 132*, 41486.

Sapuan S.M (2017) Composite materials. In: *Composite Materials Concurrent Engineering Approach*. Pp. 57-93. Elsevier Ed, United Kingdom.

Standard Test Method for Compressive Properties of Plastic Lumber and Shapes. ASTM D6108-13.

Standard Test Method for Determining the Charpy Impact Resistance of Notched Specimens of Plastics. ASTM D110-10.

Standard Test Method for Flexural Properties of Polymer Matrix Composite Materials. ASTM D7264 / D7264M-15.

StandardTest Method for Leeb Hardness Testing of Steel Products. ASTM-A956-06.

Tang L.Ch, Zhang H, Sprenger S, Ye L, Zhang Z. (2012). Fracture mechanism of epoxy-based ternary composite filled with rigid-soft particle. *Composites Science Technology 72*, 558-568.

Thoman M.R. (1999). Composite roof for a railway car, USA Patent: 5988074 A.

Zaripov R., Gavrilovs P. (2017). Research opportunities to improve technical and economic performance of freight car through the introduction of lightweight materials in their construction. *Procedia Engineer 187*, 22-29.